

Article

Evaluation of Meteorological Drought and Flood Scenarios over Kenya, East Africa

Brian Ayugi ¹, Guirong Tan ^{1,*}, Ruoyun Niu ², Zeyao Dong ³, Moses Ojara ⁴, Lucia Mumo ¹, Hassen Babaousmail ⁵ and Victor Ongoma ⁶

¹ Collaborative Innovation Center on Forecast and Evaluation of Meteorological Disasters/Key Laboratory of Meteorological Disaster, Ministry of Education, Nanjing University of Information Science and Technology, Nanjing 210044, China; ayugi.o@gmail.com (B.A.); mumolucia@gmail.com (L.M.)

² National Meteorological Centre, China Meteorological Administration, Beijing 100081, China; niury@cma.gov.cn

³ NUIST-Reading Academy, Nanjing University of Information Science and Technology, Nanjing 210044, China; 20178311035@nuist.edu.cn

⁴ Uganda National Meteorological Authority, Clement Hill Road, P.O. Box 7025 Kampala, Uganda; ojacksmoz@gmail.com

⁵ School of Computer and Software, Nanjing University of Information Science and Technology, Nanjing 210044, China; baw.hassan12@gmail.com

⁶ School of Geography, Earth Science and Environment, University of the South Pacific, Laucala Campus, Private Bag, Suva 61321, Fiji; victor.ongoma@gmail.com

* Correspondence: tanguirong@nuist.edu.cn

Received: 6 February 2020; Accepted: 20 March 2020; Published: 21 March 2020



Abstract: This work examines drought and flood events over Kenya from 1981 to 2016 using the Standardized Precipitation–Evapotranspiration Index (SPEI). The spatiotemporal analysis of dry and wet events was conducted for 3 and 12 months. Extreme drought incidences were observed in the years 1987, 2000, 2006, and 2009 for SPEI-3, whilst the SPEI-12 demonstrated the manifestation of drought during the years 2000 and 2006. The SPEI showed that the wettest periods, 1997 and 1998, coincided with the El Nino event for both time steps. SPEI-3 showed a reduction in moderate drought events, while severe and extreme cases were on the increase tendencies towards the end of the twentieth century. Conversely, SPEI-12 depicted an overall increase in severe drought occurrence over the study location with an observed intensity of -1.54 and a cumulative frequency of 64 months during the study period. Wet events showed an upward trend in the western and central highlands, while the rest of the regions showed an increase in dry events during the study period. Moreover, moderate dry/wet events predominated, whilst extreme events occurred least frequently across all grid cells. It is apparent that the study area experienced mild extreme dry events in both categories, although moderately severe dry events dominated most parts of the study area. A high intensity and frequency of drought was noted in SPEI-3, while the least occurrences of extreme events were recorded in SPEI-12. Though drought event prevailed across the study area, there was evidence of extreme flood conditions over the recent decades. These findings form a good basis for next step of research that will look at the projection of droughts over the study area based on regional climate models.

Keywords: drought; SPEI; wet; severity; frequency; duration; Kenya

1. Introduction

Drought remains one of the most complex natural phenomena affecting the economy, environment, and society at the global, regional, and local levels [1]. For instance, occurrences of prolonged rainfall

failure remarkably alter water resources and ecosystem balance, and they have adverse impacts on agriculture and urban livelihoods [2,3]. There is growing concern following the impacts of a rapidly changing climate, with projections pointing to an increase in extreme events (such as droughts and floods) that are expected to occur in across many regions [4].

Consequently, with an emphasis on drought, the focus of many researchers has been to infer from the intricate dynamics of drought and vulnerability impacts in a bid to establish mitigation measures [5–7]. Despite the efforts, according to World Meteorological Organization (WMO) [8], there is still a limited understanding of drought evolution, frequency, and severity of occurrence from one region to another. This is due to its ‘creeping phenomenon’ as compared to other natural disasters [2]. For instance, drought varies by multiple dynamic dimensions including severity and duration, making it difficult for scientists and policy makers to determine the exact timing of its inception or the termination of either meteorological, agricultural, or hydrological drought events [9–11].

Numerous studies have reported an upsurge in drought events in many regions with noticeable increases over the recent decades because of the ongoing global warming and decadal variability [4,5,12–14]. To illustrate this, drought has affected many countries in Europe [15,16], North America [17–19], Asia [20–22], Australia [23,24], and Africa [12,25,26]. Most significantly, Africa, southern Europe, and eastern Australia have recorded an increase in drought events, mostly attributed to a precipitation decrease linked with decadal fluctuations in the Pacific and western Indian Ocean [13,27,28].

East Africa (EA), mainly classified as an arid and semi-arid (ASAL) region despite falling within the tropics, continues to experience unprecedented records of drought events in comparison to other natural threats such as heat waves, torrents, cold surge, and cyclones [29,30]. Colossal records of economic losses and environmental degradation continue to be witnessed across many parts of the region [30,31]. For example, Kenya, Uganda, Somalia, and Ethiopia experienced a severe drought event in 2010–2011 [30], with an estimated 10 million people acutely impacted [31]. Furthermore, approximately 450,000 deaths were reported in Ethiopia during the 1984–1985 drought while Kenya witnessed a wide spread drought in 2005, affecting 2.5 million people in the northern region [32,33]. This trend is likely to increase with the intensification of extreme climate events towards the end of the 21st century [13,34,35]. Global predictions based on the Palmer Drought Severity Index (PDSI) show that desiccation will become more severe and widespread over the EA region with reduced precipitation and increased evaporation [13].

Kenya has been witnessing an increase in severe and frequent famine events in recent decades, exacerbated by the recent decline in March–May (MAM) seasonal rainfall [36–39]. Numerous studies have been conducted to ascertain drought variabilities, trends, and the respective impacts on agriculture, economy, water resources, and environment over the study region [40–43]. These researchers have employed various drought indices recommended by the WMO [11]. For instance, Mutsotso et al. [42] investigated the drought occurrences in Kenya based on the combination of the Standardized Precipitation–Evapotranspiration Index (SPEI) and the normalized difference vegetation index (NDVI) on a one-month basis and a three-month basis, and they analyzed correlation between the two indices. On the other hand, Karanja et al. [41] used the Standardized Precipitation Index (SPI) to characterize seasonal and annual droughts in Laikipia west sub-county, Kenya from 1984 to 2014. The study focused on drought events occurring during the two rain seasons, namely March–May (MAM) and October–December (OND). Frank et al. [44] employed the Effective Drought Index (EDI) as an “accurate” index in drought assessment in the Tana River Basin in Kenya. In contrast, Zargar et al. [45] reported contradictory results that the EDI seemed to have a weak imprecision in monitoring the inception, cessation, and accumulated stress. Wambua et al. [46] applied both the SPI and the EDI to delineate drought occurrences during 1980–2016 in the upper Tana River Basin, where nearly all the agro–ecological zones of Kenya are located. Both indices demonstrated that the southeastern parts of the basin were more likely to experience severe droughts as compared to the northwestern parts.

The mentioned indices employed by various researchers over the study domain highlighted a glimpse of spatiotemporal variation and the occurrence of historical dry/wet events from one region to another without necessarily indicating the magnitude, severity, and duration of extreme

events. Moreover, other studies on drought and flood evaluation have reported a contrary occurrence of dryness/wetness events, while some have shown incoherence in the spatial patterns of drought frequencies. Therefore, the precise analysis of recent changes in drought and wet events in a complex subtropical domain is an important step in identifying mechanisms associated with these anomalous events in the era of changing climate, which remains a challenge.

Thus, the main objective of this study was to characterize drought and wet events based on intensity, severity, and frequency at each grid cell over the Kenya from 1981 to 2016 through the use of a widely accepted and used index, the SPEI [47]. The results are useful in the accurate examination of the drought and wet events in the study locale, thereby helping hydrologists and farmers to take timely decisions. The findings of this work form a good basis for the analysis and discussion of drought projections over the region based on improved regional climate models (RCM) datasets.

The remaining sections are organized as follows: Section 2 highlights characterization of the study area, data, and methodology, while results and discussions are given in Section 3. Finally, conclusion and recommendation are presented in Section 4.

2. Materials and Methods

2.1. Study Area

Kenya is situated in East Africa. It is bound within longitude 34° E–42° E and latitude 5° S–5° N (Figure 1). Adjoining nations include Uganda, Tanzania, and Somalia. The economy of the country is predominately anchored on rain-fed agriculture [48]. Complex geomorphological features regulating local climate dominate different parts in the country. The highest altitude is in central highlands, while low-lying regions characterized by an ASAL climate and ecosystems occupies the eastern, northwest, and northeastern sides. Towards the south lies the Indian Ocean coastline regulating local climate, whereas the western sides of the study domain have a large water basin of Lake Victoria, driving land-lake breezes [49].

The rainfall of the study locale is mostly bimodal, with ‘long rains’ experienced during March to May (MAM) while ‘short rains’ occur during October to December (OND) [31,36,38,50]. Overall, a dry anomalous climate is experienced despite the region being situated along equatorial wet tropical belt. Circulation features associated with seasonal rainfall climatology over the region have been extensively elaborated on in past studies [37,49,51–57].

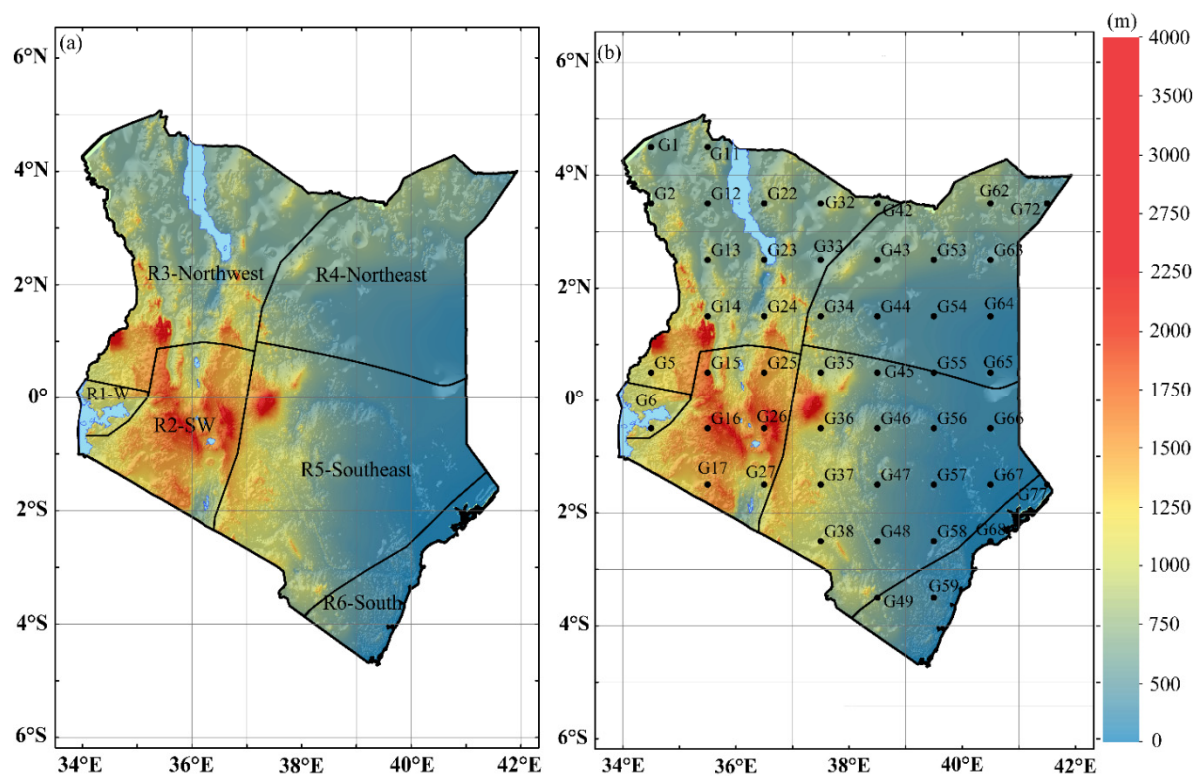


Figure 1. Elevation of the study area with distinct homogeneous locations, as delineated by Indeje et al. [58] and the respective grid cells in each region.

2.2. Data Description

The comprehensive assessment of meteorological drought and wet events over a region involves the use of several climatic datasets. This study utilized monthly maximum and minimum temperature datasets from the Climatic Research Unit (CRU TS4.03; [59]) and monthly precipitation datasets obtained from Climate Hazard Group Infrared Precipitation with Station (CHIRPS.v2; [60]).

The CHIRPS datasets were produced following two steps: (i) pentad rainfall estimates, produced from cold cloud duration (CCD)-based satellite data on a regression model calibrated with TRMM (Tropical Rainfall Measuring Mission); (ii) the stations are merged with CHIRP data to produce CHIRPS. This product has a spatial resolution of 0.05 (~5.3 km) with a quasi-global coverage (50° S–50° N, 180° E–180° W) and has existed from 1981 to present-day at pentad, decadal, and monthly temporal resolutions [60]. The study used the datasets for the period 1981 to 2016.

The CHIRPS were recently evaluated by inferring their performance over the study domain [61]. The CRU data with a spatial resolution of $\sim 50 \times 50$ km were used in deriving the potential evapotranspiration (PET). In the present study, all datasets were extracted from all grid cells within the study domain (Figure 1). This was derived by re-gridding the study area based on a $1^\circ \times 1^\circ$ spatial resolution in a bid to achieve uniform grids for analysis since the gridded datasets were of varying resolutions. An analysis at each grid cell provided an insight into the evolution of extreme events in a region that is characterized by varying topographical features on a finer horizontal resolution. This approach improves the representation of orographic features, such as elevation and land use, as well as other surface features that might not otherwise be captured in major homogeneous regions [40].

2.3. Methods and Metrics

2.3.1. Standardized Precipitation Evapotranspiration

The SPEI is computed using precipitation and the PET to delineate the phases of the anomaly of dry and wet conditions by normalizing the alteration amongst water supply (precipitation) and demand (evapotranspiration). The SPEI and the SPI [62] are almost similar except that the SPEI includes PET and employs various schemes to derive the PET. The SPEI built in the R Program language version 3.4.2 was used to compute the SPEI. Vicente-Serrano et al. [47] expounded more details on the mathematical equation for computing the SPEI.

Comparable to the original SPI, a negative value indicates dry conditions, whilst a positive value depicts wet condition [63]. For instance, drought events are divided into four main categories, namely: extreme ($\text{SPEI} \leq -2.00$), severe ($-1.50 > \text{SPEI} > -1.99$), moderate ($-1.00 > \text{SPEI} > -1.49$), and mild ($0 > \text{SPEI} > -0.99$). Similarly, wet events are categorized as follows: extreme ($\text{SPEI} \leq +2.00$), severe ($+1.50 > \text{SPEI} > +1.99$), moderate ($+1.00 > \text{SPEI} > +1.49$), and mild ($0 > \text{SPEI} > +0.99$). These values for the SPEI defines the characteristics of drought or wet conditions in terms of severity, intensity, and the duration of occurrence. In this study, the threshold of $\text{SPEI} \leq -1.0$ was inferred to signify dry events whereas $\text{SPEI} \geq +1.0$ represented wet events over the study domain. A similar threshold was employed in a recent study that examined the spatiotemporal evolution of drought in the Tana River Basin in Kenya [40].

This study defined the severity, intensity, and frequency for dry/wet events over the study domain as given in Equations (1)–(3);

- i) Severity is the cumulative sum of the index value based on the duration extent (Equation (1));

$$S = \sum_{i=1}^{\text{Duration}} \text{Index} \quad (1)$$

- ii) The intensity of an event is the severity divided by the duration (Equation (2)). Events that have shorter duration and higher severity will have large intensities.

$$I = \frac{\text{Severity}}{\text{Duration}} \quad (2)$$

- iii) The frequency of occurrence (F_s) is defined in Equation (3):

$$F_s = \frac{n_s}{N_s} \times 100\% \quad (3)$$

where n_s is the number of drought events ($\text{SPEI} < -1.0$), N_s is the total of the months for the study period, and s is a grid cell.

Furthermore, the duration of the dryness/wetness situation is presented by the length of time (months) that the drought index is consecutively above or below a truncation value. The intensity, severity, and frequency of extreme events define drought/wet episodes. The dominance of the dry/wet cases was examined for each grid cell and timescale, and it was computed on the percentage of the frequency of each incidence with reference to the total number of months. This approach was successfully employed in a recent study of drought evaluation along the major water basin in Kenya [40]. The intention of employing this approach was to categorize regions that frequently experience the concurrence of extreme and severe climatic cases at corresponding periods.

The SPEI values were calculated in two time scales, namely: SPEI-3 and SPEI-12. The SPEI-3 is derived by averaging the 3-month values, i.e., (March–May) within a year, while SPEI-12 is from

accumulated 12-month timescale. A timescale of 3 months was chosen to denote drought/flood impacts on agriculture during the crop growing season [64–66]. On the other hand, the selection of a 12-month timescale aimed to reflect the hydrological consequences of drought such as energy production services.

2.3.2. Mann–Kendall Test

The study employed the Mann–Kendall (MK) test [67,68] to detect the significance of the SPEI-3 and SPEI-12 analyses. The non-parametric feature of the MK test allows it to confirm the existence of a trend in any data against the null hypothesis of no trend. In addition, it does not require the sample to conform to any specific probability distribution since it works well even with insufficient or abnormal values. The significance of the trend was tested at the 5% significance level. A Z-score exceeding the magnitude of critical values at the 5% significance level denotes a monotonic trend of drought/flood events. The S value denotes variance, which is used to calculate the significance of the trend. Numerous hydro-climate studies across various domains have employed MK tools for trend analysis [69–72]. Moreover, Sen Slope estimator was used to detect the magnitude of the trends [73].

2.3.3. Empirical Cumulative Frequency

The empirical cumulative frequency (ECDF) [74] was adopted to compare the performance of time series for the SPEI and the SPI over the study region. The empirical cumulative frequency ($F_N(t)$) is expressed as given in Equation (4)

$$F_N(t) = \frac{1}{N} \sum_{i=1}^N 1(x_i \leq t), \quad (4)$$

where N is the number of months in observations and $(x_i \leq t)$ is the number of drought index values less than the value of t (that is, if drought index is less than t the summation adds one, otherwise zero until the total length of monthly time series). The concurrence performance of the SPI and the SPEI based on the ECDF analysis over study domain is presented in Figure 2. The results showed that the indices shared a similar frequency for all drought categories, as highlighted in Gozzo et al. [63]. For instance, the cumulative frequency for severe and extreme wet/dry events was well captured across the classifications. Besides, the robustness of the SPEI is derived from its ability to combine the various aspects of the SPI with data on evapotranspiration, qualifying it further to a substantially accurate drought index. Many evaluative studies have ranked the SPEI as the best index for drought assessment compared to other indices [75,76]. The PET employed in the present study is based on the Hargreaves scheme that relies on any available time series A datasets and has superior performance similar to that of the Food and Agricultural Organization (FAO) criterion of Pen-Monteith [77]. Comparative studies examining the suitability of different PET estimations over diverse domains have found a better performance of the PET derived from the Hargreaves equation with a cautionary point regarding difference in few hundred-of-millimeter scale across different locations or characterized by unique land cover [78]. Thus, the present study employed SPEI indices for the historical trends synthesis of drought at each grid pixel over the study domain. The SPI is recommended for drought/flood events analysis in situations where minimum (maximum) temperature datasets that could be used for the aid in computing the evapotranspiration for the SPEI are missing or unavailable.

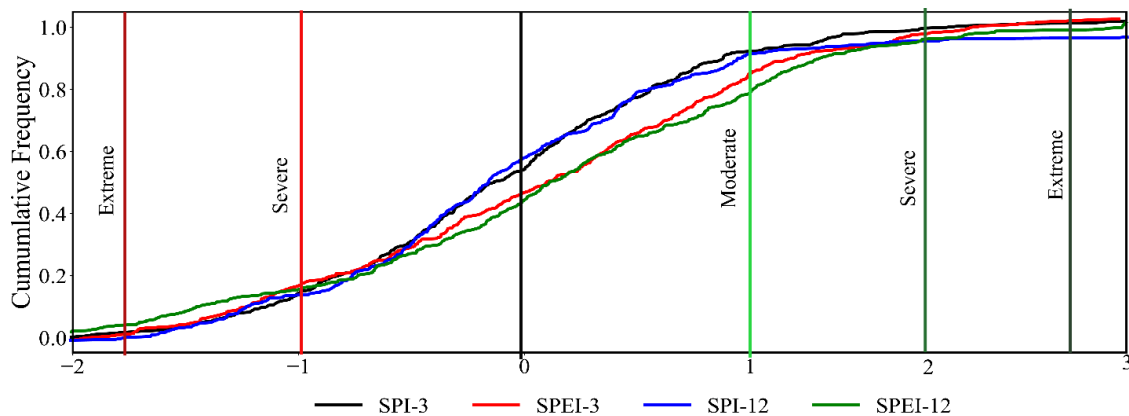


Figure 2. The empirical cumulative frequency of the monthly Standardized Precipitation Index (SPI) and the Standardized Precipitation–Evapotranspiration Index (SPEI) for the Kenya region. Vertical lines represent the dry spell (red) and wet spell (green) thresholds, classified in drought indices presented by Gozzo et al. [63].

3. Results

3.1. Temporal Patterns and Frequency Incidences of Dry/Wet Events

Figure 3 provides an overview of historical analysis for SPEI 3- and 12-month for the years 1981 to 2016 over Kenya. In addition, the Mann–Kendall test statistics for SPEI-3 and SPEI-12 analysis over study domain are presented in Table 1. The evaluation of drought and wet events was conducted for moderate, severe, and extreme frequencies [47,79]. From the SPEI-3 results (Figure 3a), it can be seen that the study domain experienced moderate-to-severe and moderate-to-extreme drought cases towards the end of the twentieth century. The SPEI-3 for both wet and dry events showed an increasing trend at the 5% significance level (Table 1). The results agree with the observed abrupt shift in rainfall tendency that occurred in the late 1990s from wet years to an almost continuous period with well-below average rainfall over the study domain [26,39,80]. This trend has been consistent in the three decades following the early 1980s, and a series of very dry years prevailed around 2010 [37]. The extreme drought incidences were observed during the years 1987, 2000, 2006, and 2009 for SPEI-3. The listed years coincide with atmospheric circulation changes related to sea surface temperature (SST) variations that influence the regional rainfall patterns [27]. Further, the observed changes in drought characteristic for the SPEI-3 event indicated a moderate intensity phenomenon at -1.43 , although the severity recorded was more intense with noted value of -111.5 over the duration of 78 months (Table 2). It is apparent from results presented that SPEI-3 exhibited a greater temporal frequency of the occurrence of wet and dry cases during the study duration. This could be explained by the fact that SPEI-3 represented an average of months in which region received a maximum rainfall amount characterized by a high variability from one region to another.

The results for SPEI-12 showed stability in the frequency of incidences over the study area during the period of 1981–2016. This demonstrates that the SPEI at elongated timescales responded gradually and consistently to deviations in climatic variables, indicating strong durations of frequent occurrences of anomalous events over the years. Subsequently, the longer timescales were most appropriate for the revealing of the incidences of signature events over the region, whereas shorter intervals demonstrated a suitability for detecting frequent seasonal and inter-annual variations. The further analysis of drought severity (Figure 3c) show an overall severe drought occurrence over the study location with an observed intensity of -1.54 and a cumulative frequency of 64 months during the study period (Table 2). The extreme drought incidences were observed during the years 2000 and 2006. A significant test at 5% significance revealed a decreasing trends for SPI-12 wet years, while dry years showed opposite increasing tendencies (Table 1). Overall decreasing patterns in wet events

were mainly influenced by the observed decreases in rainfall over the study area during the recent decades [26,36–38].

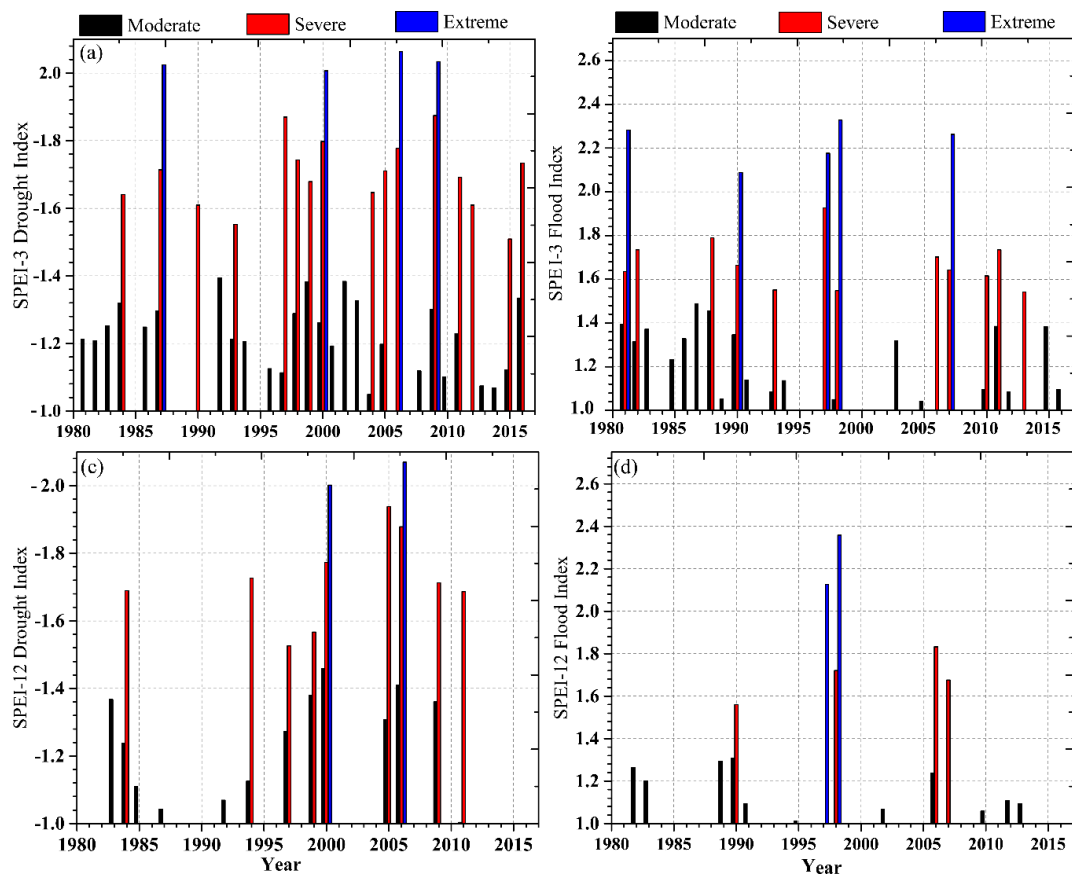


Figure 3. Evolution of the mean SPEI for 3- and 12-month timescales for moderate, severe, and extreme drought and flood over Kenya showing the variation in the duration, severity, and intensity of dry and wet events, 1981–2016.

Table 1. Summary of Mann–Kendall test statistic for SPEI-3 and SPEI-12 over Kenya at the 5% significance level.

| Trend Analysis | SPEI-Test | | | |
|----------------|---------------------------|---------------------------|---------------------------|---------------------------|
| | SPEI-3 Dry | SPEI-3 Wet | SPEI-12 Dry | SPEI-12 Wet |
| S | 3150 | 1130 | 2080 | −1170 |
| Z | 13.12 | 11.38 | 11.77 | −11.77 |
| p | <0.0001 | <0.0001 | <0.0001 | <0.0001 |
| Alpha | 0.05 | 0.05 | 0.05 | 0.05 |
| significance | Significant Increasing | Significant Increasing | Significant Increasing | Significant Decreasing |

Negative (positive) Z-values indicate a significantly or insignificantly decreasing (increasing) trend.

Table 2. The duration, severity, and intensity occurrence of the major dry (SPEI ≤ −1) and wet (SPEI ≥ 1) events over Kenya during 1981–2016.

| Event | SPEI | Duration | Severity | Intensity |
|-------|------|----------|----------|-----------|
| Dry | 3 | 78 | −111.15 | −1.43 |
| | 12 | 64 | −98.70 | −1.54 |
| Wet | 3 | 61 | 94.79 | 1.55 |
| | 12 | 61 | 93.31 | 1.53 |

A comparison of the two indices showed that SPEI-3 was characterized by severe drought occurrence, while long-term drought (SPEI-12) showed a reduction in the extreme events over the study area. Meanwhile, the wetness episodes for both SPEI-3/12 demonstrated a severe occurrence with an intensity of $\text{SPEI} \geq 1.5$ in all intervals. The wettest period between 1997 and 1998 during the El Niño event was well captured in both time steps, depicting a robust performance of the SPEI in capturing the underlying mechanisms of wet conditions. A comparison of the two results revealed an overall moderate dry condition occurrence, while more intense wet events over the short duration of existence were experienced.

Further evaluations for the SPEI were conducted over six homogeneous climatic zones, as delineated by Indeje et al. [58]. The SPEI values for each region were identified by averaging the values at each grid cell, as presented in Figure 1. The regions are as follows: R1—western sides; R2—southwest; R3—northwest; R4—northeast; R5—southeast; and R6—south coastal area. Figures 4 and 5 demonstrate the linear trend for the dry and wet events for different time scales across the six regions during the period of 1981–2016. It is worth noting that in both timescales, the R1 and R2 depicted increasing trends in wet events, while the rest of the regions showed increases in dry events during the study period. R1 and R2 were characterized by high elevations, while R3, R4, and R5 were mostly occupied by the bare lands of the arid and semi-arid climates. These regions experienced below-normal rainfall and high temperature, resulting in a high evapotranspiration as compared to R1 and R2, which were characterized by a dense vegetation cover and a raised water table. Moreover, the high terrains in R1 and R2 produced lee rain shadows and blocked the passing of rain-bearing disturbances in other regions [81]. An in-depth analysis at each grid cell along the homogenous zones was conducted based on duration, severity, and magnitude of occurrences of some significant anomalous incidences. Table 3 highlights the evolution of dry/wet events for some noteworthy cases over the study region. The dry/wet years highlighted concurred with similar years, as noted over the whole area average (Figure 3).

The results from the analyses of the frequency of wet and dry events for SPEI-3 for all grids pixels across the study domain demonstrated that moderate events predominated and extreme events occurred less frequently across all grid cells during the study period. It was further noted that variations of wet/dry events occurred across different grid cells from one-time scale to another. This agreed with previous studies that observed similar variations of anomalous climate events across different parts of the study domain [41–43,82]. For instance, the wettest event for SPEI-3 was recorded in grid cell 58 during May 1981, and the duration for occurrence lasted for 87 months. Likewise, the prolonged duration of the dry event for SPEI-3 was observed in pixels 36 and 49 and lasted for 83 months. Regarding the severity of the below and above normal events over the study domain, Table 3 gives locations that had experienced these abnormal climatic cases. The most severe dry event for SPEI-3 was remarked in grid cell 36. More notably, the severe wet event was experienced over similar grid cell 36 with a magnitude of 125.95. This showed that the region experienced both extremes as compared to other regions over the study domain, a feature worth further investigation.

The findings for SPEI-12 based on individual grid cells for the analysis of wet and dry event frequency demonstrate that moderate events prevailed and extreme events occurred less frequently across all grid cells during the study period. The wettest event for SPEI-12 was experienced March 1998 in grid cells 34 and 55 with the duration of occurrence persisting for 97 months. A drought analysis demonstrated a prolonged duration of a dry event in grid cell 7 for 82 months. Concerning the severity of the below and above normal events over the study domain, Table 3 show that the most severe dry event for SPEI-12 ensued in pixel 62. On the contrary, the severe wet event was noted over grid cells 17 and 63 with a magnitude of 119. Overall, the moderate intensity of both wet and dry events for SPE-3 and 12 was experienced across the study domain during the study duration except for grid cell 55, which recorded a high intensity of $\text{SPEI} \geq 1.5$. This agreed with previous studies conducted over various parts of the study domain or based on different indices [42,83,84].

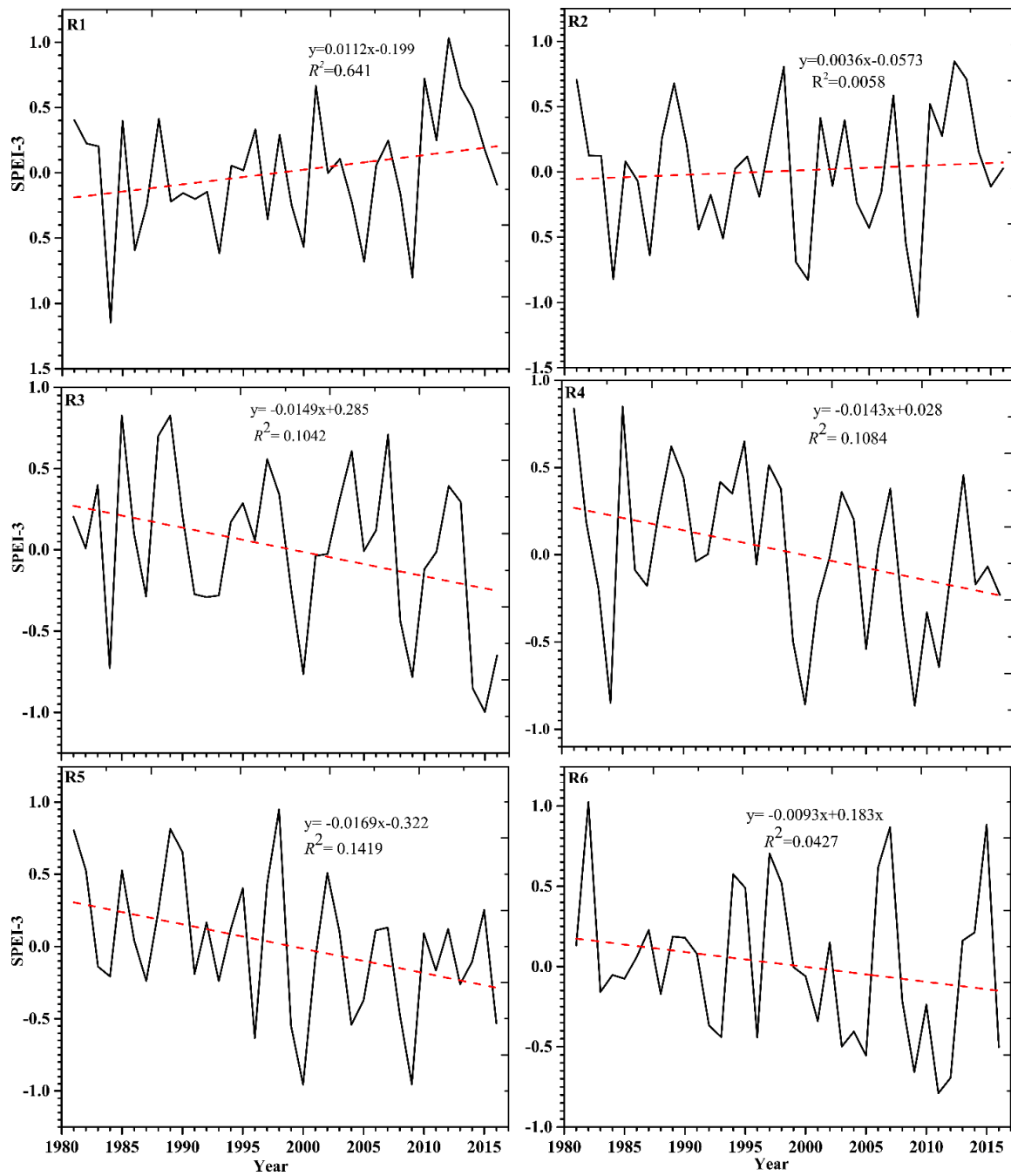


Figure 4. Linear trends of dry and wet events for SPEI-3 over six distinct climatic zones, as presented in Figure 1.

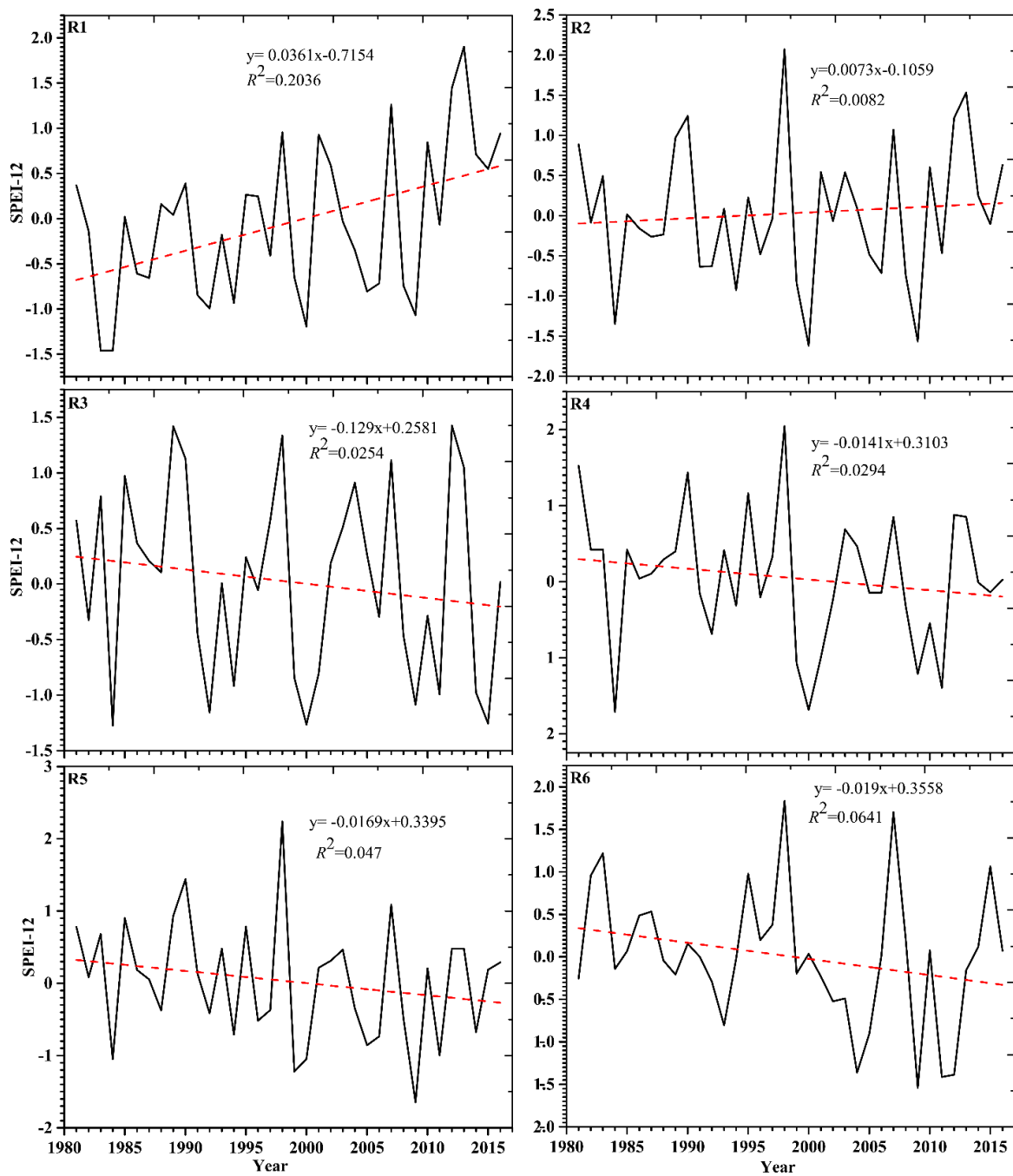


Figure 5. Linear trends of dry and wet events for SPEI-12 over six distinct climatic zones, as presented in Figure 1.

Table 3. The duration, severity and intensity of occurrence of some of the major dry and wet events (SPEI \leq -1 SPEI \geq +1) over each grid cell in Kenya, 1981–2016.

| Grid | Duration | Severity | Intensity | Grid | Duration | Severity | Intensity |
|------------------------------|----------|----------|-----------|------------------------------|----------|----------|-----------|
| Dry Event for SPEI-3 | | | | Wet Event for SPEI-3 | | | |
| 4 | 80 | -110.74 | -1.38 | 4 | 81 | 115.69 | 1.42 |
| 15 | 81 | -109.76 | -1.35 | 26 | 80 | 117.26 | 1.46 |
| 16 | 81 | -109.74 | -1.35 | 44 | 85 | 121.71 | 1.43 |
| 27 | 82 | -114.28 | -1.39 | 48 | 81 | 117.61 | 1.45 |
| 36 | 83 | -114.81 | -1.38 | 72 | 87 | 125.92 | 1.44 |
| 49 | 83 | -112.69 | -1.35 | 73 | 80 | 119.58 | 1.49 |
| 67 | 80 | -107.9 | -1.34 | 76 | 80 | 116.05 | 1.45 |
| Dry Event for SPEI-12 | | | | Wet Event for SPEI-12 | | | |
| 7 | 82 | -112.69 | -1.37 | 7 | 81 | 111.65 | 1.37 |
| 13 | 80 | -112.28 | -1.40 | 27 | 80 | 116.22 | 1.45 |
| 17 | 78 | -110.48 | -1.41 | 32 | 85 | 119.88 | 1.41 |
| 36 | 76 | -107.69 | -1.41 | 38 | 81 | 115.89 | 1.43 |
| 48 | 78 | -108.77 | -1.39 | 47 | 80 | 113.5 | 1.42 |
| 55 | 79 | -108.21 | -1.36 | 53 | 97 | 97.59 | 1.54 |
| 62 | 78 | -113.83 | -1.45 | 58 | 81 | 115.83 | 1.43 |
| 63 | 77 | -112.19 | -1.45 | 77 | 87 | 119.4 | 1.37 |

3.2. Spatial Patterns of SPEI in the Study Area

The spatial pattern of the frequency of severe and extreme dry (wet) cases for the SPEI-3 and SPEI-12 months periods are presented in Figures 6 and 7, respectively. From the analysis introduced in Figure 6, it is apparent that the study area experienced mild extreme dry events in both categories, whilst moderately severe dry events dominated the most parts of the domain. For instance, the frequency of severe dry events for SPEI-3 varied from 3.25 in grid cell 72 to 6.51 in pixel 57, situated in the northeastern region. On the other hand, extreme dry events depicted a uniform distribution over the study locale with low incidences during SPEI-3. The percentage occurrence ranged from 0.23 in grid cell 27 and 36 to 3.72 in grid cell 53, along the northeastern area. Moreover, maximum frequency was recorded in pixel 63 with a percentage value of 1.86. Overall, a high intensity and frequency of drought were noted during SPEI-3.

Analyses for severe and extreme wet events are presented in Figure 7. The wet events were mainly found in the western parts, extending towards southern sides and partly central areas during the severe wet events for SPEI-3, while extreme wetness covered most parts of the study domain. The frequency of severe wet events for SPEI-3 varied from 3.25 in grid cells 59 and 50 to 7.9 in pixel 5, situated in the western region. On the other hand, a maximum frequency was recorded in pixel 59 with a percentage value of 3.25, whereas a minimum wet event was observed over grid 6 along Lake Victoria, with a recorded value of 0.46.

Meanwhile, an assessment for SPEI-12 revealed the occurrence of maximum severe dry events observed in grid cell 42 (8.6) characterized by ASAL ecosystems, while the least severe dry scenario was recorded over in grid 77 (2.09) along the coastal region. Over ASAL areas, anomalous soil moisture content restrains dehydration, and little vegetation cover reduces transpiration rates, results in a low mean latent heat flux as compared to over humid lands [6]. Extreme dry events depicted a bimodal distribution over the study locale with the fewest occurrences of extreme events recorded during the study duration.

The severity and extreme wet events are presented in Figure 7. The wet events were mainly noted in the western parts, extending towards southern sides and partly central areas during the severe wet events, while strong wetness was observed over the northeastern region during the SPEI-12 timescales. The frequency of severe wet events for SPEI-12 was observed in grid cell 16 (9.06), while the minimum severe wet event observed over most grids, namely 64, 65, and 43 (0.23), situated along the northeastern

sides. Meanwhile, extreme wet events had a percentage occurrence ranging from 0.23 over grid cell 23 to 4.18 in grid cell 34.

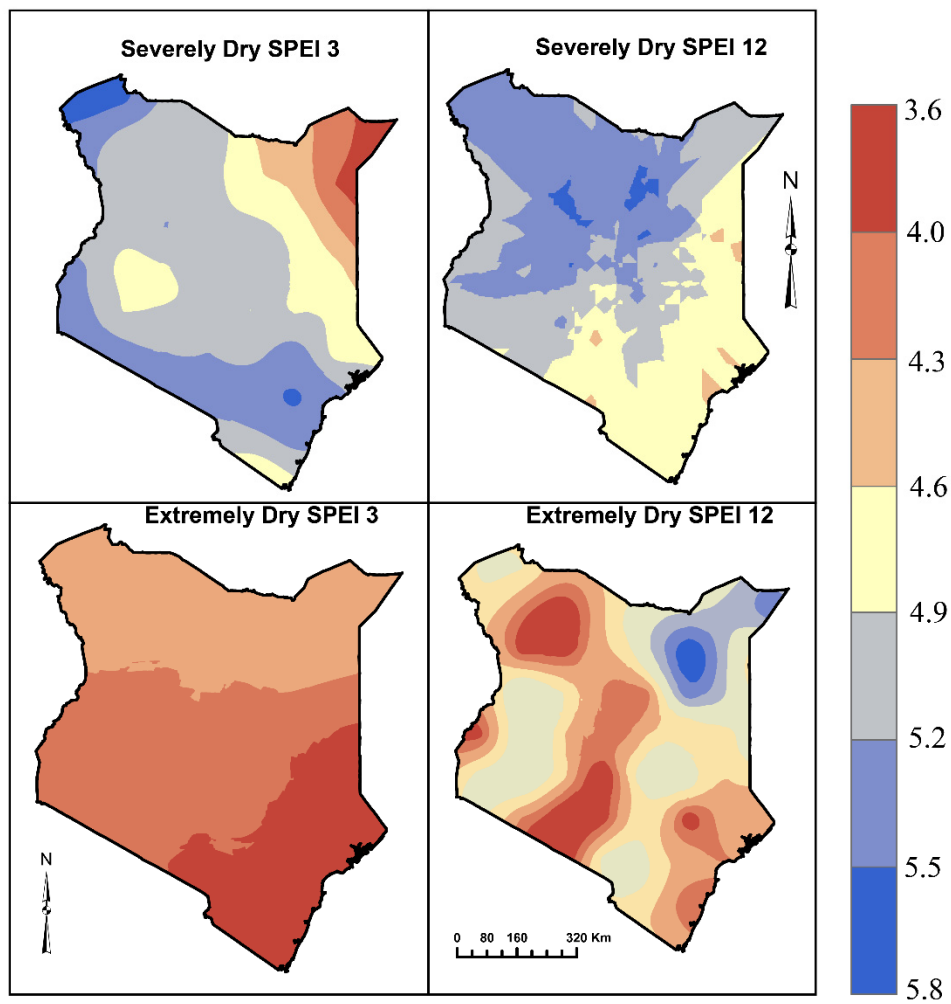


Figure 6. Frequency of severe (**top**) and extreme (**bottom**) dry events computed for SPEI-3 and SPEI-12, respectively, over Kenya, 1981–2016.

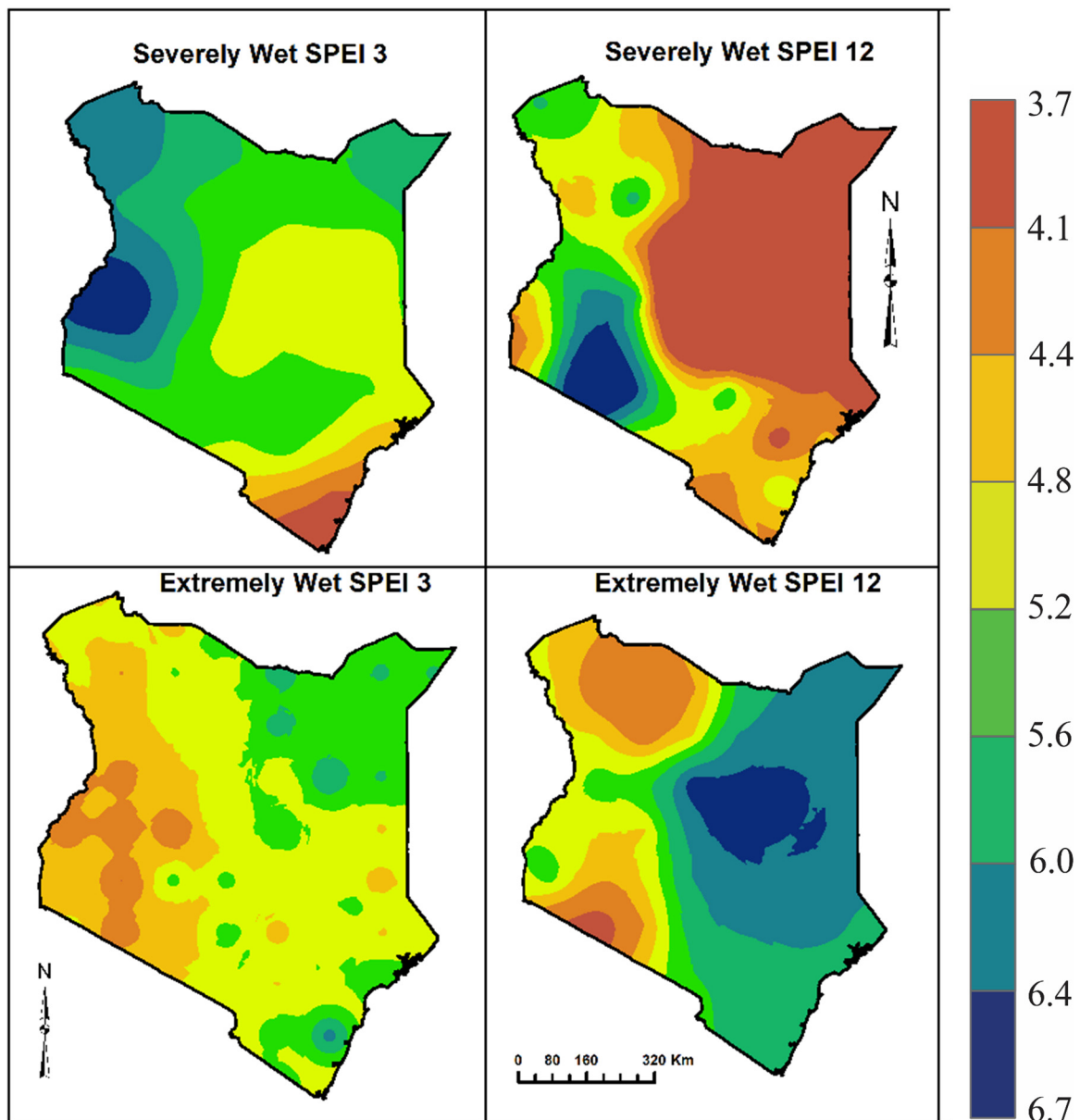


Figure 7. Frequency of severe (**top**) and extreme (**bottom**) wet events computed for the SPEI-3 and SPEI-12 month respectively over Kenya, 1981–2016.

4. Discussion

Drought occurrence is a stochastic natural phenomenon that is mainly influenced from changes in climatic variables, namely precipitation and temperature. The variability of both variables from historical perspective has been observed in a number of existing studies with a sharp increase being noted, most significantly in temperature towards the end of the 20th century and the beginning of the 21st century era [34]. It is worth remarking that the observed trends towards the end of 21st century were mainly as a result of GHG-induced changes and changes caused by internal variability, e.g., by ENSO and the Interdecadal Pacific Oscillation (IPO) [29,85–87]. This is equally echoed in a recent Intergovernmental Panel on Climate Change (IPCC) report that stated an unequivocal warming from 1950s across the globe as a result of anthropogenic-induced global warming [4]. The observed variability in climatic variables is likely to have had a profound impact in the drought/flood mechanism over the study domain, which is influenced by ratio of precipitation and potential evapotranspiration [29,88,89]. For instance, an increase in surface air temperature towards the end of the 21st century will likely

significantly influence the PET levels that characterize the evaporative demand of the atmosphere. Other factors include low humidity and abundant solar radiation, which remains a signature feature over the study domain [90].

As a consequence of global warming, there is apprehension that increased temperature, which is linked to evapotranspiration, may lead to increase in drought incidences and severity across many regions [12,13,91,92]. The study domain has been experiencing rapid increase of trends in extreme events, characterized by drought and wet scenarios towards end of the 20th century and the beginning of the 21st century (Table 1). While the drought event has prevailed, there are extreme flood conditions with devastating consequences that have been equally witnessed [31]. Evidently, the severity and intensity of drought/flood, along with abrupt deviations between the extremes, continues to pose a threat to the livelihoods of people; hence, the need for continuous evaluation of drought and flood occurrences over the study domain remains paramount.

The results of this present study that examined meteorological drought and wet scenarios over Kenya with a robust index of the SPEI during study the duration (Figure 3), points to decreasing patterns in moderate wetting occurrences towards the end of the twentieth century, a result that is also in harmony with past studies [39,80,93]. Moreover, the impact of drought has been shown to vary from low-lying regions to humid vegetative areas (Figures 4 and 5), predominantly due to surface and atmospheric interaction dynamics. For example, the changes in wet events is mostly associated with the heightened heating of the SST of the Indian Ocean, which alters the Walker circulation anomalies contributing to drying trends [27]. On the other hand, the recent drying tendency over the study domain (Table 3) could have been because of changes in the tropical SSTs variations over the Indo-Pacific [39,91]. This may have led to a substantial increase in regional aridity and drought areas [12,13]. In addition, the large-scale atmospheric circulation changes associated with a weaker West African monsoon may likely have contributed [26,27]. Consequently, this could negatively affect the area's economy that entirely relies on season-based farming for livelihoods and sustainability [48,80].

This study thus highlights key features of drought and wet events, which remain the major climatic extremes that affect people and property [94,95]. Understanding the historical complexities and dynamics of drought and flood events could build the momentum to conduct further studies on the future evolution of these extreme events over the study area, with a view of recommending appropriate and timely policies to avert damages and loss of life. This study reveals the occurrences of mild extreme dry events, whilst moderately severe dry events dominated most parts of the domain (Figures 6 and 7). The high intensity and frequency of drought were noted in SPEI-3, whereas the least occurrences of extreme events were recorded in SPEI-12.

5. Conclusions

Drought remains one of the most complex natural phenomena affecting the economy, environment, and society at the global, regional, and local levels. The present study examined drought and wet events by characterizing the trends, intensity, severity, and frequencies based on widely accepted indices of the SPEI over Kenya, East Africa from 1981 to 2016. The spatial and temporal evolution of dry and wet events was captured by both a 3- and 12-month SPEI. Extreme drought incidences were observed during the years 1984, 1987, 2000, 2006, and 2009 for SPEI-3, whilst for SPEI-12, drought manifested during the years 2000 and 2006. The wettest period was noted in 1997–1998 and was attributed to a strong El Nino event. This shows how well the SPEI performed in capturing the underlying mechanisms of dry/wet conditions.

SPEI-3 showed an occurrence of moderate-to-severe and moderate-to-extreme drought cases towards the end of the twentieth century, whilst SPEI-12 depicted an overall increase in severe drought occurrence over the study location with an observed intensity of -1.54 and a cumulative frequency of 64 months during the study period. Spatial patterns showed that the western and central highlands had an increasing trend in wet events, while the rest of the regions showed an increase in dry events

during the study period. Moreover, moderate dry/wet events were dominant, while extreme events occurred least frequently across all grid cells during the study period.

It is apparent that during the study duration, the region experienced mild extreme dry events in both categories, whilst moderate-to-severe dry events dominated most parts of the domain. A high intensity and frequency of drought were noted in SPEI-3, whilst least occurrences of extreme events were recorded in SPEI-12. Where a drought event has prevailed, there have been extreme flood conditions with possible devastating consequences equally witnessed.

Author Contributions: Conceptualization, B.A. and V.O.; methodology, M.O. and B.A.; software, M.O.; validation, L.M., H.B., and B.A.; formal analysis, B.A. and G.T.; investigation, G.T., R.N., V.O., and B.A.; resources, G.T. and R.N.; data curation, B.A. and M.O.; writing—original draft preparation, B.A. and Z.D.; writing—review and editing, G.T., V.O., L.M., and B.A.; visualization, M.O., H.B., and B.A.; supervision, G.T.; project administration, G.T., B.A., and R.N.; funding acquisition, G.T. and R.N. All authors have read and agreed to the published version of the manuscript.

Funding: National Key Research and Development Program of China (2018YFC1507703&2016YFA0600702), National Natural Science Foundation of China (41575070 and 41575085) supported this work

Acknowledgments: The authors acknowledge Nanjing University of Information Science and Technology (NUIST) for providing favorable environment and infrastructural needs for conducting research. Special appreciation to all data centers for availing data to use for evaluation studies. The lead author is grateful to NUIST for granting him scholarship to pursue PhD studies. The four anonymous reviewers are highly appreciated for the great input that led to the massive improvement of this manuscript.

Conflicts of Interest: In a unanimous agreement, all authors declare no conflict of interest in the present study.

References

1. Parsons, D.J.; Rey, D.; Tanguy, M.; Holman, I.P. Regional variations in the link between drought indices and reported agricultural impacts of drought. *Agric. Syst.* **2019**, *173*, 119–129. [[CrossRef](#)]
2. Wilhite, D.A. Chapter 1 Drought as a natural hazard: Concepts and definitions. In *Drought Mitigation Center Faculty Publications*; Routledge: London, UK, 2000; p. 69.
3. Rohli, R.V.; Bushra, N.; Lam, N.S.; Zou, L.; Mihunov, V.; Reams, M.A.; Argote, J.E. Drought indices as drought predictors in the south-central USA. *Nat. Hazards* **2016**, *83*, 1567–1582. [[CrossRef](#)]
4. IPCC. *Climate Change 2014: Synthesis Report. Contribution of Working Groups I, II and III to the Fifth Assessment Report of the Intergovernmental Panel on Climate Change*; Pachauri, R.K., Meyer, L.A., Eds.; IPCC: Geneva, Switzerland, 2014; p. 151.
5. Sheffield, J.; Wood, E.F.; Roderick, M.L. Little change in global drought over the past 60 years. *Nature* **2012**, *491*, 435. [[CrossRef](#)]
6. Huang, J.; Li, Y.; Fu, C.; Chen, F.; Fu, Q.; Dai, A.; Wang, G. Dryland climate change: Recent progress and challenges. *Rev. Geophys.* **2017**, *55*, 719–778. [[CrossRef](#)]
7. Wang, G.; Gong, T.; Lu, J.; Lou, D.; Hagan, D.F.T.; Chen, T. On the long-term changes of drought over China (1948–2012) from different methods of potential evapotranspiration estimations. *Int. J. Climatol.* **2018**, *38*, 2954–2966. [[CrossRef](#)]
8. WMO. Experts Recommend Agricultural Drought Indices for improved understanding of food production conditions. In *Developments in Earth Surface Processes*; WMO: Murcia, Spain, 2010; Press Release No. 887.
9. Wilhite, D.A.; Glantz, M.H. Understanding: The drought phenomenon: The role of definitions. *Water Int.* **1985**, *10*, 111–120. [[CrossRef](#)]
10. Łabędzki, L. Estimation of local drought frequency in central Poland using the standardized precipitation index SPI. *Irrig. Drain. J. Int. Comm. Irrig. Drain.* **2007**, *56*, 67–77. [[CrossRef](#)]
11. WMO; GWP. *Handbook of Drought Indicators and Indices*; Svoboda, M., Fuchs, B.A., Eds.; Integrated Drought Management Programme (IDMP), Integrated Drought Management Tools and Guidelines Series 2; WMO: Geneva, Switzerland, 2016.
12. Dai, A. Characteristics and trends in various forms of the Palmer Drought Severity Index during 1900–2008. *J. Geophys. Res. Atmos.* **2011**, *116*. [[CrossRef](#)]
13. Dai, A. The influence of the inter-decadal Pacific oscillation on US precipitation during 1923–2010. *Clim. Dyn.* **2013**, *41*, 633–646. [[CrossRef](#)]

14. Trenberth, K.E.; Dai, A.; van der Schrier, G.; Jones, P.D.; Barichivich, J.; Briffa, K.R. Global warming and changes in drought. *Nat. Clim. Chang.* **2014**, *4*, 17. [[CrossRef](#)]
15. Spinoni, J.; Naumann, G.; Vogt, J.V.; Barbosa, P. The biggest drought events in Europe from 1950 to 2012. *J. Hydrol. Reg. Stud.* **2015**, *3*, 509–524. [[CrossRef](#)]
16. Bradford, R. *Drought Events in Europe, in Drought and Drought Mitigation in Europe*; Springer: Berlin/Heidelberg, Germany, 2000; pp. 7–20.
17. Cook, E.R.; Seager, R.; Cane, M.A.; Stahle, D. North American drought: Reconstructions, causes, and consequences. *Earth Sci. Rev.* **2007**, *81*, 93–134. [[CrossRef](#)]
18. Schwalm, C.R.; Seager, R.; Cane, M.A.; Stahle, D.W. Reduction in carbon uptake during turn of the century drought in western North America. *Nat. Geosci.* **2012**, *5*, 551. [[CrossRef](#)]
19. AghaKouchak, A.; Cheng, L.; Omid, M.; Alireza, F. Global warming and changes in risk of concurrent climate extremes: Insights from the 2014 California drought. *Geophys. Res. Lett.* **2014**, *41*, 8847–8852. [[CrossRef](#)]
20. Cai, Q.; Liu, Y.; Liu, H.; Ren, J. Reconstruction of drought variability in North China and its association with sea surface temperature in the joining area of Asia and Indian–Pacific Ocean. *Palaeogeogr. Palaeoclimatol. Palaeoecol.* **2015**, *417*, 554–560. [[CrossRef](#)]
21. Liang, L.; Zhao, S.H.; Qin, Z.H.; Ke-Xun, H.E.; Chong, C.; Luo, Y.X.; Zhou, X.D. Drought change trend using MODIS TVDI and its relationship with climate factors in China from 2001 to 2010. *J. Integr. Agric.* **2014**, *13*, 1501–1508. [[CrossRef](#)]
22. Sun, S.; Chen, H.; Wang, G.; Li, J.; Mu, M.; Yan, G.; Zhu, S. Shift in potential evapotranspiration and its implications for dryness/wetness over Southwest China. *J. Geophys. Res. Atmos.* **2016**, *121*, 9342–9355. [[CrossRef](#)]
23. Chiew, F.H.S.; Potter, N.J.; Vaze, J.; Petheram, C.; Zhang, L.; Teng, J.; Post, D.A. Observed hydrologic non-stationarity in far south-eastern Australia: Implications for modelling and prediction. *Stoch. Environ. Res. Risk Assess.* **2014**, *28*, 3–15. [[CrossRef](#)]
24. Rahmat, S.N.; Jayasuriya, N.; Bhuiyan, M. Development of drought severity-duration-frequency curves in Victoria, Australia. *Australas. J. Water Resour.* **2015**, *19*, 31–42. [[CrossRef](#)]
25. Hulme, M. Rainfall changes in Africa: 1931–1960 to 1961–1990. *Int. J. Climatol.* **1992**, *12*, 685–699. [[CrossRef](#)]
26. Lyon, B.; DeWitt, D.G. A recent and abrupt decline in the East African long rains. *Geophys. Res. Lett.* **2012**, *39*. [[CrossRef](#)]
27. Hua, W.; Zhou, L.; Chen, H.; Nicholson, S.E.; Raghavendra, A.; Jiang, Y. Possible causes of the Central Equatorial African long-term drought. *Environ. Res. Lett.* **2016**, *11*, 124002. [[CrossRef](#)]
28. Dai, A.; Zhao, T. Uncertainties in historical changes and future projections of drought. Part I: Estimates of historical drought changes. *Clim. Chang.* **2017**, *144*, 519–533. [[CrossRef](#)]
29. Lyon, B. Seasonal drought in the Greater Horn of Africa and its recent increase during the March–May long rains. *J. Clim.* **2014**, *27*, 7953–7975. [[CrossRef](#)]
30. Gebremeskel, G.; Tang, Q.; Sun, S.; Huang, Z.; Zhang, X.; Liu, X. Droughts in East Africa: Causes, impacts and resilience. *Earth Sci. Rev.* **2019**, *193*, 146–161. [[CrossRef](#)]
31. Nicholson, S.E. The predictability of rainfall over the Greater Horn of Africa. Part I: Prediction of seasonal rainfall. *J. Hydrometeorol.* **2014**, *15*, 1011–1027. [[CrossRef](#)]
32. Guha-Sapir, D.; Hargitt, D.; Hoyois, P. *Thirty Years of Natural Disasters 1974–2003: The Numbers*; Presses universitaires de Louvain: Louvain, Belgium, 2004.
33. Balint, Z.; Mutua, F.; Muchiri, P.; Omuto, C.T. Monitoring drought with the combined drought index in Kenya. In *Developments in Earth Surface Processes*; Elsevier: Berlin/Heidelberg, Germany, 2013; pp. 341–356.
34. Ongoma, V.; Chen, H.; Gao, C. Projected changes in mean rainfall and temperature over East Africa based on CMIP5 models. *Int. J. Climatol.* **2018**, *38*, 1375–1392. [[CrossRef](#)]
35. Rowell, D.P.; Booth, B.B.B.; Nicholson, S.E.; Good, P. Reconciling past and future rainfall trends over East Africa. *J. Clim.* **2015**, *28*, 9768–9788. [[CrossRef](#)]
36. Ongoma, V.; Chen, H. Temporal and spatial variability of temperature and precipitation over East Africa from 1951 to 2010. *Meteorol. Atmos. Phys.* **2017**, *129*, 131–144. [[CrossRef](#)]
37. Ayugi, B.O.; Tan, G.; Ongoma, V.; Mafuru, K.B. Circulations associated with variations in boreal spring rainfall over Kenya. *Earth Syst. Environ.* **2018**, *2*, 421–434. [[CrossRef](#)]
38. Mumo, L.; Yu, J.; Ayugi, B. Evaluation of spatiotemporal variability of rainfall over Kenya from 1979 to 2017. *J. Atmos. Sol. -Terr. Phys.* **2019**, *194*, 105097. [[CrossRef](#)]

39. Williams, A.P.; Funk, C. A westward extension of the warm pool leads to a westward extension of the Walker circulation, drying eastern Africa. *Clim. Dyn.* **2011**, *37*, 2417–2435. [[CrossRef](#)]
40. Polong, F.; Chen, H.; Sun, S.; Ongoma, V. Temporal and spatial evolution of the standard precipitation evapotranspiration index (SPEI) in the Tana River Basin, Kenya. *Theor. Appl. Climatol.* **2019**, *138*, 777–792. [[CrossRef](#)]
41. Karanja, A.; Ondimu, K.; Recha, C. Analysis of Temporal Drought Characteristic Using SPI Drought Index Based on Rainfall Data in Laikipia West Sub-County, Kenya. *Open Access Libr. J.* **2017**, *4*, 1–11. [[CrossRef](#)]
42. Mutsotso, R.B.; Sichangi, A.W.; Makokha, G.O. Spatio-Temporal Drought Characterization in Kenya from 1987 to 2016. *Adv. Remote Sens.* **2018**, *7*, 125. [[CrossRef](#)]
43. Changwony, C.; Sichangi, A.W.; Ngigi, M.M. Using GIS and Remote Sensing in Assessment of Water Scarcity in Nakuru County, Kenya. *Adv. Remote Sens.* **2017**, *6*, 88. [[CrossRef](#)]
44. Frank, A.; Armenski, T.; Gocic, M.; Popov, S.; Popovic, L.; Trajkovic, S. Influence of mathematical and physical background of drought indices on their complementarity and drought recognition ability. *Atmos. Res.* **2017**, *194*, 268–280. [[CrossRef](#)]
45. Zargar, A.; Sadiq, R.; Naser, B.; Khan, F.I. A review of drought indices. *Environ. Rev.* **2011**, *19*, 333–349. [[CrossRef](#)]
46. Wambua, R.M.; Mutua, B.M.; Raude, J.M. Detection of Spatial, Temporal and Trend of Meteorological Drought Using Standardized Precipitation Index (SPI) and Effective Drought Index (EDI) in the Upper Tana River Basin, Kenya. *Open J. Mod. Hydrol.* **2018**, *8*, 83. [[CrossRef](#)]
47. Vicente-Serrano, S.M.; Beguería, S.; López-Moreno, J.I. A multiscale drought index sensitive to global warming: The standardized precipitation evapotranspiration index. *J. Clim.* **2010**, *23*, 1696–1718. [[CrossRef](#)]
48. Mumo, L.; Yu, J.; Fang, K. Assessing Impacts of Seasonal Climate Variability on Maize Yield in Kenya. *Int. J. Plant Prod.* **2018**, *12*, 297–307. [[CrossRef](#)]
49. Camberlin, P. Climate of Eastern Africa. In *Oxford Research Encyclopedia of Climate Science*; Oxford University Press USA: New York, NY, USA, 2018.
50. Ayugi, B.O.; Wen, W.; Chepkemoi, D. Analysis of spatial and temporal patterns of rainfall variations over Kenya. *J. Env. Earth Sci.* **2016**, *6*, 69–83.
51. Ogwang, B.A.; Chen, H.; Tan, G.; Ongoma, V.; Ntwali, D. Diagnosis of East African climate and the circulation mechanisms associated with extreme wet and dry events: A study based on RegCM4. *Arab. J. Geosci.* **2015**, *8*, 10255–10265. [[CrossRef](#)]
52. Kinuthia, J.; Asnani, G. A newly found jet in North Kenya (Turkana Channel). *Mon. Weather Rev.* **1982**, *110*, 1722–1728. [[CrossRef](#)]
53. Hastenrath, S.; Polzin, D.; Camberlin, P. Exploring the predictability of the ‘short rains’ at the coast of East Africa. *Int. J. Climatol. A J. R. Meteorol. Soc.* **2004**, *24*, 1333–1343. [[CrossRef](#)]
54. Indeje, M.; Semazzi, F. Relationships between QBO in the lower equatorial stratospheric zonal winds and East African seasonal rainfall. *Meteorol. Atmos. Phys.* **2000**, *73*, 227–244. [[CrossRef](#)]
55. Nicholson, S.E. Climate and climatic variability of rainfall over eastern Africa. *Rev. Geophys.* **2017**, *55*, 590–635. [[CrossRef](#)]
56. Pohl, B.; Crétat, J.; Camberlin, P. Testing WRF capability in simulating the atmospheric water cycle over Equatorial East Africa. *Clim. Dyn.* **2011**, *37*, 1357–1379. [[CrossRef](#)]
57. Hastenrath, S. Zonal circulations over the equatorial Indian Ocean. *J. Clim.* **2000**, *13*, 2746–2756. [[CrossRef](#)]
58. Indeje, M.; Semazzi, F.H.; Ogallo, L.J. ENSO signals in East African rainfall seasons. *Int. J. Climatol.* **2000**, *20*, 19–46. [[CrossRef](#)]
59. Harris, I.; Jones, P.D.; Osborn, T.J.; Lister, D.H. Updated high-resolution grids of monthly climatic observations—the CRU TS3.10 Dataset. *Int. J. Climatol.* **2014**, *34*, 623–642. [[CrossRef](#)]
60. Funk, C.; Peterson, P.; Landsfeld, M.; Pedreros, D.; Verdin, J.; Shukla, S.; Michaelsen, J. The climate hazards infrared precipitation with stations—A new environmental record for monitoring extremes. *Sci. Data* **2015**, *2*, 150066. [[CrossRef](#)] [[PubMed](#)]
61. Ayugi, B.; Tan, G.; Ullah, W.; Boiyo, R.; Ongoma, V. Inter-comparison of remotely sensed precipitation datasets over Kenya during 1998–2016. *Atmos. Res.* **2019**, *225*, 96–109. [[CrossRef](#)]
62. McKee, T.B.; Doesken, N.J.; Kleist, J. The relationship of drought frequency and duration to time scales. In Proceedings of the 8th Conference on Applied Climatology, Anaheim, CA, USA, 17–22 January 1993; American Meteorological Society Boston: Boston, MA, USA, 1993.

63. Gozzo, L.F.; Palma, D.S.; Custodio, M.S.; Machado, J.P. Climatology and Trend of Severe Drought Events in the State of Sao Paulo, Brazil, during the 20th Century. *Atmosphere* **2019**, *10*, 190. [[CrossRef](#)]
64. Balint, Z.; Mutua, F.; Muchiri, P. *Drought Monitoring with the Combined Drought Index*; FAO-SWALIM: Nairobi, Kenya, 2011; pp. 3–25.
65. Hayes, M.J.; Svoboda, M.D.; Wilhite, D.A.; Vanyarkho, O.V. Monitoring the 1996 drought using the standardized precipitation index. *Bull. Am. Meteorol. Soc.* **1999**, *80*, 429–438. [[CrossRef](#)]
66. Manatsa, D.; Mukwada, G.; Siziba, E.; Chinyanganya, T. Analysis of multidimensional aspects of agricultural droughts in Zimbabwe using the Standardized Precipitation Index (SPI). *Theor. Appl. Climatol.* **2010**, *102*, 287–305. [[CrossRef](#)]
67. Mann, H.B. Nonparametric tests against trend. *Econom. J. Econom. Soc.* **1945**, *13*, 245–259. [[CrossRef](#)]
68. Kendall, M. *Rank Correlation Methods*, 4th ed.; Charles Griffin: San Francisco, CA, USA, 1975; Volume 8.
69. Ayugi, B.; Tan, G.; Gnitou, G.T.; Ojara, M.; Ongoma, V. Historical evaluations and simulations of precipitation over East Africa from Rossby centre regional climate model. *Atmos. Res.* **2020**, *232*, 104705. [[CrossRef](#)]
70. Ongoma, V.; Chen, H.; Gao, C. Evaluation of CMIP5 twentieth century rainfall simulation over the equatorial East Africa. *Theor. Appl. Climatol.* **2018**, *135*, 893–910. [[CrossRef](#)]
71. Araghi, A.; Mousavi-Baygi, M.; Adamowski, J. Detection of trends in days with extreme temperatures in Iran from 1961 to 2010. *Theor. Appl. Climatol.* **2016**, *125*, 213–225. [[CrossRef](#)]
72. Ayugi, B.O.; Tan, G. Recent trends of surface air temperatures over Kenya from 1971 to 2010. *Meteorol. Atmos. Phys.* **2019**, *131*, 1401–1413. [[CrossRef](#)]
73. Sen, P.K. Estimates of the regression coefficient based on Kendall's tau. *J. Am. Stat. Assoc.* **1968**, *63*, 1379–1389. [[CrossRef](#)]
74. Zambreski, Z.T. A statistical assessment of drought variability and climate prediction for Kansas. Ph.D. Thesis, Kansas State University, Manhattan, Kansas, 2016.
75. Mumo, L.; Yu, J. Gauging the performance of CMIP5 historical simulation in reproducing observed gauge rainfall over Kenya. *Atmos. Res.* **2020**, *236*, 104808. [[CrossRef](#)]
76. Lorenzo-Lacruz, J.; Vicente-serrano, S.M.; López-moreno, J.I.; Beguería, S.; García-ruiz, J.M. The impact of droughts and water management on various hydrological systems in the headwaters of the Tagus River (central Spain). *J. Hydrol.* **2010**, *386*, 13–26. [[CrossRef](#)]
77. Allen, R.G.; Pereira, L.D.; Raes, D.; Smith, M. Crop evapotranspiration-Guidelines for computing crop water requirements-FAO Irrigation and drainage paper 56. *Fao Rome* **1998**, *300*, D05109.
78. Federer, C.; Vörösmarty, C.; Fekete, B. Intercomparison of methods for calculating potential evaporation in regional and global water balance models. *Water Resour. Res.* **1996**, *32*, 2315–2321. [[CrossRef](#)]
79. Beguería, S.; Vicente-Serrano, S.M.; Reig, F.; Latorre, B. Standardized precipitation evapotranspiration index (SPEI) revisited: Parameter fitting, evapotranspiration models, tools, datasets and drought monitoring. *Int. J. Climatol.* **2014**, *34*, 3001–3023. [[CrossRef](#)]
80. Funk, C.; Dettinger, M.D.; Michaelsen, J.C.; Verdin, J.P.; Brown, M.E.; Barlow, M.; Hoell, A. Warming of the Indian Ocean threatens eastern and southern African food security but could be mitigated by agricultural development. *Proc. Natl. Acad. Sci. USA* **2008**, *105*, 11081–11086. [[CrossRef](#)]
81. Ogwang, B.A.; Chen, H.; Li, X.; Chujie, G. The influence of topography on East African October to December climate: Sensitivity experiments with RegCM4. *Adv. Meteorol.* **2014**, *2014*, 143917. [[CrossRef](#)]
82. Awange, J.L.; Aluoch, J.; Ogallo, L.A.; Omulo, M.; Omondi, P. Frequency and severity of drought in the Lake Victoria region (Kenya) and its effects on food security. *Clim. Res.* **2007**, *33*, 135–142. [[CrossRef](#)]
83. Mwangi, E.; Wetterhall, F.; Dutra, E.; Di Giuseppe, F.; Pappenberger, F. Forecasting droughts in East Africa. *Hydrol. Earth Syst. Sci.* **2014**, *18*, 611–620. [[CrossRef](#)]
84. Nicholson, S.E. A detailed look at the recent drought situation in the Greater Horn of Africa. *J. Arid Environ.* **2014**, *103*, 71–79. [[CrossRef](#)]
85. Gu, G.; Adler, R.F. Interdecadal variability/long-term changes in global precipitation patterns during the past three decades: Global warming and/or pacific decadal variability? *Clim. Dyn.* **2013**, *40*, 3009–3022. [[CrossRef](#)]
86. Dai, A. Future warming patterns linked to today's climate variability. *Sci. Rep.* **2016**, *6*, 19110. [[CrossRef](#)] [[PubMed](#)]
87. Dong, B.; Dai, A. The influence of the interdecadal Pacific oscillation on temperature and precipitation over the globe. *Clim. Dyn.* **2015**, *45*, 2667–2681. [[CrossRef](#)]

88. Hulme, M. Climate change within the period of meteorological records. In *The Physical geography of Africa*; Oxford University Press: Oxford, UK, 1996; pp. 88–102.
89. Feng, S.; Fu, Q. Expansion of global drylands under a warming climate. *Atmos. Chem. Phys.* **2013**, *13*, 14637–14665. [[CrossRef](#)]
90. Ji, M.; Huang, J.; Xie, Y.; Liu, J. Comparison of dryland climate change in observations and CMIP5 simulations. *Adv. Atmos. Sci.* **2015**, *32*, 1565–1574. [[CrossRef](#)]
91. Liebmann, B.; Hoerling, M.P.; Funk, C.; Bladé, I.; Dole, R.M.; Allured, D.; Quan, X.; Pegion, P.; Eischeid, J.K. Understanding recent eastern Horn of Africa rainfall variability and change. *J. Clim.* **2014**, *27*, 8630–8645. [[CrossRef](#)]
92. Wang, L.; Yuan, X.; Xie, Z.; Wu, P.; Li, Y. Increasing flash droughts over China during the recent global warming hiatus. *Sci. Rep.* **2016**, *6*, 30571. [[CrossRef](#)]
93. Tierney, J.E.; Ummenhofer, C.C.; deMenocal, P.B. Past and future rainfall in the Horn of Africa. *Sci. Adv.* **2015**, *1*, e1500682. [[CrossRef](#)]
94. Zhang, X.; Chen, N.; Sheng, H.; Ip, C.; Yang, L.; Chen, Y.; Sang, Z.; Tadesse, T.; Lim, T.P.; Rajabifard, A.; et al. Urban drought challenge to 2030 sustainable development goals. *Sci. Total Environ.* **2019**, *693*, 133536. [[CrossRef](#)] [[PubMed](#)]
95. Dilling, L.; Daly, M.E.; Kenney, D.A.; Klein, R.; Miller, K.; Ray, A.J.; Travis, W.R.; Wilhelmi, O. Drought in urban water systems: Learning lessons for climate adaptive capacity. *Clim. Risk Manag.* **2019**, *23*, 32–42. [[CrossRef](#)]



© 2020 by the authors. Licensee MDPI, Basel, Switzerland. This article is an open access article distributed under the terms and conditions of the Creative Commons Attribution (CC BY) license (<http://creativecommons.org/licenses/by/4.0/>).